Local Maxwell Tomography Using Transmit-Receive Coil Arrays for Contact-Free Mapping of Tissue Electrical Properties and Determination of Absolute RF Phase

Daniel K. Sodickson[1,2], Leeor Alon[1,2], Cem Murat Deniz[1,2], Ryan Brown[1], Bei Zhang[1], Graham C. Wiggins[1], Gene Y. Cho[1,2], Noam Ben Eliezer[1], Dmitry S. Novikov[1], Riccardo Lattanzi[1,2], Qi Duan[3], Lester A. Sodickson[4], and Yudong Zhu[1,2]

[1]*Bernard and Irene Schwartz Center for Biomedical Imaging, Department of Radiology, New York University School of Medicine, New York, NY, United States,* [2]*Sackler Institute of Graduate Biomedical Sciences, New York University School of Medicine, New York, NY, United States,* [3]*National Institutes of Health, Bethesda, MD, United States,* [4]*Cambridge Research Associates, Newton, MA, United States*

Introduction: Knowledge of the spatial distribution of electrical conductivity and permittivity is valuable both as an adjunct for various diagnostic and therapeutic technologies (e.g. for TMS, RF ablation, or *in vivo* SAR mapping in high-field MRI), and perhaps even more as a new window on the microstructure and function of tissues and materials, complementary to that provided by traditional imaging modalities. Recently, magnetic resonance has begun to play a key enabling role in noninvasive electrical property mapping, for example by providing internal information to overcome the ill-conditioned inverse problem of surface-based electrical impedance tomography[1]. A new approach, electrical properties tomography (EPT)[2], achieves noninvasive mapping without injected currents, using measurements of magnetic field curvature to deduce electrical property distributions. Results with EPT to date have been highly promising, with early *in vivo* studies in patient populations just emerging[3]. However, EPT, and any prospective field-curvature-related technique, suffers from a fundamental lack of access to absolute RF phase, as all measurable phases are expressed in relation to some unknown reference phase distribution[4]. EPT circumvents this limitation to some extent by using a carefully-chosen coil design (a birdcage) and associated symmetry assumptions dictating field behavior in the body. These assumptions fail preferentially at high field strength – precisely where field curvature is greatest and electrical property maps would otherwise be expected to be most effective and most valuable (e.g. for local SAR determination). Here, we introduce a new general technique called Local Maxwell Tomography (LMT) which is free of assumptions regarding RF phase and coil/field/magnetization structure. LMT solves simultaneously for key functions of the missing RF phase distribution along with unknown electrical properties, using complementary information from the transmit and receive sensitivity distributions of multiple coils to resolve ambiguities. LMT, from which EPT may be derived as a special case, enables electrical property mapping at arbitrary field strength, with a wide range of coil designs, and free of errors associated with rapid field variation.

Methods: *Electrodynamics:* Defining time-harmonic electromagnetic fields $\mathbf{B}(\mathbf{r},t)=\mathbf{B}(\mathbf{r})\exp(-i\omega t)$ and $\mathbf{E}(\mathbf{r},t)=\mathbf{E}(\mathbf{r})\exp(-i\omega t)$ with angular frequency ω, manipulation of Maxwell's equations results in the following local expression relating field curvature to conductivity σ and permittivity ε: $\nabla^2\mathbf{B}=-i\omega\mu(\sigma-i\omega\varepsilon)\mathbf{B}-\nabla\{\mu(\sigma-i\omega\varepsilon)\}\times\mathbf{E}\xrightarrow{\text{slowly varying }\sigma,\varepsilon}-i\omega\mu(\sigma-i\omega\varepsilon)\mathbf{B}$. If we can measure the curvature of any Cartesian component of the laboratory-frame magnetic field, or any linear combination of such components, we can determine electrical properties as a function of position. *Measurables:* With MR, we have access to quantities related to the right and left circularly polarized magnetic field components $B_1^{(\pm)}$ via transmit and receive field mapping, however absolute phase and magnetization distribution remain inaccessible to us. The pure field maps on which we would like to operate may be expressed in terms of known (blue) and unknown (red) quantities as follows: $B_{1,l}^{(+)}=\left(\left|B_{1,l}^{(+)}\right|\exp(i\varphi_{\Sigma_l})\right)\left(\exp(-i\varphi_0)\right)$ and $B_{1,l'}^{(-)}=\left(\left|MB_{1,l'}^{(-)}\right|\exp(i\varphi_{\Delta_{l'}})\right)\left(|M|^{-1}\exp(+i\varphi_0)\right)$. Here, φ_0 is the unknown phase distribution associated with a chosen reference receive coil or coil combination, and $|M|$ is the unknown distribution of magnetization. l labels transmit coils, and l' receive coils. Note that φ_{Σ_l}, the sum of transmit phase and reference phase, is known from the MR signal, which involves a product of functions of transmit and receive sensitivities[5], whereas $\varphi_{\Delta_{l'}}$ the difference of receive phase and reference phase, is known from the relative phase of receive sensitivities (obtainable from quotients of measurable quantities). A B_1 mapping technique of choice may be used to map absolute magnitude $\left|B_{1,l}^{(+)}\right|$, and the quantity $\left|MB_{1,l'}^{(-)}\right|$ is derivable from this map combined with the MR signal. *Inverse problem and solution:* A product rule expansion of $\nabla^2B_1^{(\pm)}$, and separation into real and imaginary parts, results in matrix equations such as the following, with one distinct row for each transmit coil l and each receive coil l':

$$\begin{bmatrix}-2\partial\ln\left|B_{1,l}^{(+)}\right|/\partial x & -2\partial\ln\left|B_{1,l}^{(+)}\right|/\partial y & -2\partial\ln\left|B_{1,l}^{(+)}\right|/\partial z & -1 & 1\\ 2\partial\ln\left|MB_{1,l'}^{(-)}\right|/\partial x & 2\partial\ln\left|MB_{1,l'}^{(-)}\right|/\partial y & 2\partial\ln\left|MB_{1,l'}^{(-)}\right|/\partial z & 1 & 1\end{bmatrix}\begin{bmatrix}\partial\varphi_0/\partial x & \partial\varphi_0/\partial y & \partial\varphi_0/\partial z & \nabla^2\varphi_0 & \omega\mu\sigma\end{bmatrix}^T \underset{|M|}{\overset{\text{constant}}{=}}\begin{bmatrix}-2\nabla\ln\left|B_{1,l}^{(+)}\right|\cdot\nabla\varphi_{\Sigma_l}-\nabla^2\varphi_{\Sigma_l}\\ -2\nabla\ln\left|MB_{1,l'}^{(-)}\right|\cdot\nabla\varphi_{\Delta_{l'}}-\nabla^2\varphi_{\Delta_{l'}}\end{bmatrix} \quad (1)$$

This is a linear equation, and may be solved in a least-squares sense using a Moore-Penrose pseudoinverse, whose noise and error propagation behavior is well-defined. The key to determination of the gradient and Laplacian of φ_0 is to combine information from transmit and receive coils, whose conjugate relationship to the missing reference phase renders the matrix in Eq. (1) nonsingular and enables unique solution. A total of at least 5 field maps, taken from at least one transmit and at least one receive coil, is required to fix the values of the 5 unknowns in Eq. (1). A similar equation may be derived for permittivity, sharing four φ_0-related unknowns with Eq. (1). Thus, a 3-element transmit-receive array will suffice to determine both σ and ε, and larger numbers of elements will improve robustness. One may also generalize to solve for gradients of unknown magnetization distribution, increasing the number of unknowns to 10, and introducing a minor nonlinearity which does not impede unique solution. Note that Eq. (1) and all the LMT master equations are local, and may be solved voxel by voxel in parallel. *Practical issues and implementation:* Any suitable numerical derivative algorithm may be selected to compute the matrix and vector elements in the LMT master equations. We used second-order Savitsky-Golay (SG) derivatives with kernel size of 5 to 7 in all three dimensions around each voxel. In order to avoid derivative estimation errors in regions of excessively rapid field variation for any given coil, we used a local matched filter field recombination approach in which known phase relations between transmit and receive fields were used to ensure constructive interference and to create synthetic coil sets with slow field variation at the center of each SG kernel. *Experimental parameters:* A multiecho modified actual flip angle imaging (AFI) sequence[6] was used for volumetric multi-coil B_1 mapping as well as B_0 mapping to remove background non-electrodynamic phase. A low-flip-angle GRE sequence was used to generate MR signals for sum and difference phase as well as $\left|MB_{1,l'}^{(-)}\right|$ determination. Experiments were performed on a 7T whole-body MR scanner equipped with 8 transmit channels and 32 receive channels (Siemens Medical Solutions, Erlangen, Germany).

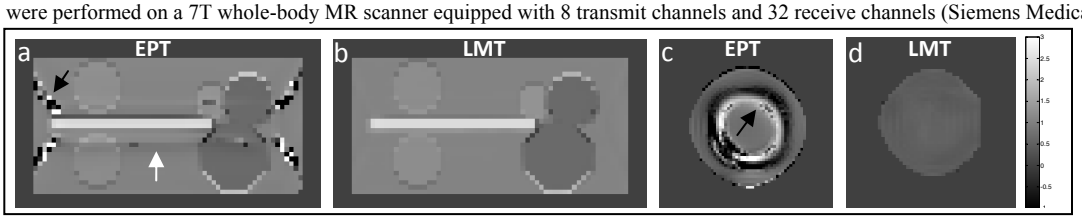

Results: ***Figure 1:*** *Conductivity maps at 7 Tesla field strength.* Panels **a** and **b** show simulations comparing EPT (a, birdcage) with LMT (b, birdcage rungs used as 16 individual elements) in a simplified cylindrical body model with heart, lung, spinal cord, kidney, and muscle compartments. Arrows show artifacts due to derivative errors (black arrow) and EPT phase assumption errors (white arrow), which are removed by LMT. Panels **c** and **d** show results of 7T experiments comparing EPT (c, birdcage) with LMT (d, encircling loop array with 8 transmit and 16 receive elements) in a single-compartment cylindrical phantom. Ring artifacts (black arrow) in EPT due to a null in birdcage sensitivity and corresponding derivative errors are removed by LMT, which yields correct electrical property values (validated by dielectric probe) as well as a correct spatial distribution. Additional results in structured phantoms and *in vivo* will be presented.

Discussion and Conclusions: LMT enables noninvasive electrical property mapping without assumptions regarding phase and field structure. Other recently described techniques[7,8] have aimed at solution of the absolute RF phase problem, but unlike LMT these techniques continue to rely on key symmetry assumptions for magnetization or field/phase distribution, thereby sacrificing full generality. As may be seen in Fig. 1 a and b, edge artifacts appear in LMT, as they do in EPT, at boundaries between regions of distinct electrical properties, but various approaches to addressing this constraint are under investigation. LMT requires additional scan time as compared with simpler approaches such as EPT, since multi-element B_1 and MR signal maps are needed. In return, in addition to being exact and free of symmetry assumptions, LMT offers increased flexibility and robustness, effectively enabling synthesis of ideal coils or fields at each spatial position of interest. As a general formalism, moreover, LMT enables one to probe the limits of simpler approaches, and to explore new and robust approximate methods.

References: [1]Seo JK et al, *J Phys Conf Ser* 2005: 12; 140. [2]Katscher U et al, *IEEE Trans Med Imaging* 2009;28:1365. [3]Voigt T et al, ISMRM 2011, 127. [4]Wiesinger F et al, *Morning Course on Unsolved Problems and Unmet Needs in Magnetic Resonance*, ISMRM 2006. [5]Hoult DI, *Concepts Magn Reson* 2000;12:173. [6]Amadon A et al, ISMRM 2008, 1248. [7]Zhang X et al, ISMRM 2011, 126. [8]Katscher U et al, ISMRM 2011, 494.